Time Course of Apoptotic Tumor Response After a Single Dose of Chemotherapy: Comparison with ^{99m}Tc-Annexin V Uptake and Histologic Findings in an Experimental Model

Toshiki Takei, MD[1]; Yuji Kuge, PhD[2]; Songji Zhao, MD[2]; Masayuki Sato, BS[3]; H. William Strauss, MD[4]; Francis G. Blankenberg, MD[5]; Jonathan F. Tait, PhD[6]; and Nagara Tamaki, MD[1]

[1]Department of Nuclear Medicine, Graduate School of Medicine, Hokkaido University, Sapporo, Japan; [2]Department of Tracer Kinetics, Graduate School of Medicine, Hokkaido University, Sapporo, Japan; [3]Department of Radiopharmaceutical Chemistry, Health Sciences University of Hokkaido, Tobetsu, Japan; [4]Department of Nuclear Medicine, Memorial Sloan–Kettering Cancer Center, New York, New York; [5]Division of Nuclear Medicine, Department of Radiology, Stanford University School of Medicine, Stanford, California; and [6]Department of Laboratory Medicine, University of Washington, Seattle, Washington

In tumors the process of apoptosis occurs over an interval of time after chemotherapy. To determine the best timing for detecting apoptosis in vivo with ^{99m}Tc-annexin V after chemotherapy, we examined the changes in ^{99m}Tc-annexin V accumulation over time in comparison with those of caspase-3 and terminal deoxynucleotidyl transferase-mediated deoxyuridine triphosphate nick-end labeling (TUNEL) expression level after cyclophosphamide treatment in an experimental model. **Methods:** Hydrazinonicotinamide (HYNIC)-annexin V was labeled with ^{99m}Tc (^{99m}Tc-annexin V). Rats were inoculated with allogenic hepatoma cells (KDH-8) into the left calf muscle. Eleven days after the inoculation, the rats were randomly divided into the group receiving a single dose of cyclophosphamide (150 mg/kg intraperitoneally) and the control group. ^{99m}Tc-Annexin V (18.5 MBq [0.5 mCi] per rat) was injected intravenously in the rats 4, 12, and 20 h after the treatment and also to the control rats (n = 5 in each group). Radioactivity in tissues was determined 6 h after ^{99m}Tc-annexin V injection. Immunostaining of caspase-3 and TUNEL were performed to detect apoptosis, and the rates of positively stained cells were calculated. **Results:** ^{99m}Tc-Annexin V accumulation in tumors significantly increased at 20 h (0.077 ± 0.007 [%ID/g] × kg, where %ID/g = percentage injected dose per gram) but not at 4 or 12 h (0.048 ± 0.008 and 0.052 ± 0.014 [%ID/g] × kg, respectively) after cyclophosphamide treatment. ^{99m}Tc-Annexin V accumulation in tumors and the rate of apoptotic cells determined by caspase-3 immunostaining and TUNEL were significantly higher in treated rats 20 h after cyclophosphamide treatment as compared with control rats. **Conclusion:** The effective detection of apoptotic tumor response with ^{99m}Tc-annexin V required 20 h after cyclophosphamide treatment in an experimental model. The present results provide an important basis for determining the best timing of annexin V imaging after the start of chemotherapy in a clinical setting.

Key Words: ^{99m}Tc-annexin V; apoptosis; cancer chemotherapy

J Nucl Med 2004; 45:2083–2087

Apoptosis plays an important role in both normal physiology and many disease processes (*1–5*). One of the earliest events in apoptosis is the externalization of phosphatidylserine (PS), a membrane phospholipid normally restricted to the inner leaflet of the lipid bilayer (*6*). Annexin V, a human protein with a high affinity for membrane-bound PS (*6–11*), has been labeled with fluorescent markers for the in vitro detection of apoptotic cells (*10,11*) and with radioactive agents, such as ^{99m}Tc, for in vivo apoptosis detection (*12–16*).

In tumor tissue, successful chemotherapy or radiotherapy induces apoptosis of neoplastic cells as a response to the therapy (*13,17–19*). Cyclophosphamide, a kind of alkylating agent, is a broad-spectrum cytotoxic agent that induces an apoptotic reaction to proliferating cells, including hepatoma (*12,20*). Previous studies demonstrated that radiolabeled annexin imaging can detect apoptosis in vivo in experimental models (*4,12–14,21–26*) of many kinds of disease and therapy. We previously reported that ^{99m}Tc-annexin V uptake in tumors significantly increased after a single dose of cyclophosphamide, and the increase was concordant with the number of terminal deoxynucleotidyl transferase-mediated deoxyuridine triphosphate nick-end labeling (TUNEL)-positive cells in tumors (*20*)—for instance, head and neck cancers, lung cancers, and malignant lymphomas (*27–29*). The current series of experiments were performed to determine the relationship of PS expression to the time after initial treatment to define the best timing for imaging with ^{99m}Tc-annexin V after the initiation of che-

Received Jan. 28, 2004; revision accepted Jul. 22, 2004.

For correspondence or reprints contact: Nagara Tamaki, MD, Department of Nuclear Medicine, Graduate School of Medicine, Hokkaido University, Kita 15 Nishi 7, Kita-ku, Sapporo 060-8638, Japan.

E-mail: natamaki@med.hokudai.ac.jp

motherapy (*27*). Accordingly, we examined the changes in ^{99m}Tc-annexin V accumulation over time in comparison with those of caspase-3 and TUNEL expression level after cyclophosphamide treatment in an experimental model.

MATERIALS AND METHODS

Preparation of Animal Models

All procedures involving animals were performed in accordance with institutional guidelines (Guide for the Care and Use of Laboratory Animals of Hokkaido University). Male Wistar King Aptekman/Hok (WKA/H) rats (supplied by the Experimental Animal Institute, Graduate School of Medicine, Hokkaido University, Sapporo) were inoculated with a suspension of KDH-8 rat hepatoma cells (1×10^6 cells per rat) into the left calf muscle (*20,30*). Eleven days after the intramuscular injection of KDH-8 cells, rats weighting 209–287 g were randomly divided into the groups receiving a single dose of cyclophosphamide (150 mg/kg, intraperitoneally) (treated group, $n = 15$) and the control group ($n = 5$). At the time of study, the tumors were approximately 14 mm in average diameter.

^{99m}Tc-Annexin V Uptake in Tumor and Biodistribution

Human annexin V was produced by expression in *Escherichia coli* as previously described (*9,10,13,16,31–33*). Annexin V was labeled with ^{99m}Tc after derivatization with hydrazinonicotinamide (HYNIC) (^{99m}Tc-annexin V; specific activity, 3.0 MBq/μg protein). HYNIC, a nicotinic acid analog, can make bridging between a target protein and ^{99m}Tc (*13,16*). ^{99m}Tc-Annexin V (3.8 μg protein per rat) was injected intravenously 4, 12, and 20 h after treatment ($n = 5$ at each time point). The group division was performed on the basis of our previous result and the pharmacokinetic character of cyclophosphamide (*34*). The animals were under light ether anesthesia at the time of injection. Six hours after ^{99m}Tc-annexin V injection, the animals were sacrificed and the tumor, blood, and other tissues were excised. The tissue samples were weighed and the radioactivity was determined with a well-type scintillation counter (1480 WizardTM3″; Wallac Co.). Tumor samples were divided into 3 parts. Then, using aliquots of the tumor tissues, formalin-fixed paraffin-embedded specimens were prepared for subsequent histologic studies. The accumulation of ^{99m}Tc-annexin V in the tissues was expressed as the percentage injected dose per gram of tissue after normalization to the animal's weight ([%ID/g] × kg). The tumor-to-muscle ratio (T/M ratio) and the tumor-to-blood ratio (T/B ratio) were calculated from the (%ID/g) × kg value in each tissue (*20,30*).

Detection of Apoptosis

Apoptotic cells were determined by hematoxylin–eosin staining, by direct immunoperoxidase detection of digoxigenin-labeled 3′ DNA strand breaks by use of TUNEL, and by immunostaining of caspase-3. The formalin-fixed paraffin-embedded tissues were sectioned at 3-μm thickness. TUNEL was performed according to a standard procedure using a commercially available kit (Apoptosis In Situ Detection Kit; Wako Pure Chemical Industries, Ltd.). Caspase-3 immunostaining was performed using antihuman/mouse caspase-3 active antibody (Genzyme/Techne). TUNEL-positively stained cells were counted in 10 randomly selected high-power (×200) fields with the observer unaware of the treatment, to avoid experimental bias (*20,30*). The rate of positively stained cells was determined by calculating the average percentage.

Statistical Analysis

All values are expressed as mean ± SD. Statistical analyses were performed using the Kruskal–Wallis test to detect the significance of difference among groups by time and the unpaired Student *t* test to evaluate the significance of differences in values between the control and treated animals (*20*).

RESULTS

The tissue distribution of radioactivity after chemotherapy is summarized in Table 1. The accumulations of ^{99m}Tc-annexin V in tumor tissue 4, 12, and 20 h after cyclophosphamide treatment were 0.048 ± 0.008, 0.052 ± 0.014, and 0.077 ± 0.007 (%ID/g) × kg, respectively. The accumulation of ^{99m}Tc-annexin V in tumor in the treated group 20 h after treatment was significantly higher than that in the control group (0.050 ± 0.010 [%ID/g] × kg, $P < 0.05$). The

TABLE 1
Biodistribution of ^{99m}Tc-Annexin V

Biodistribution	Time after cyclophosphamide treatment (h) ($n = 5$)				P (K–W)
	0 (control)	4	12	20	
Blood	0.039 ± 0.006	0.041 ± 0.005	0.041 ± 0.007	0.037 ± 0.001	NS
Tumor	0.050 ± 0.010	0.048 ± 0.008	0.052 ± 0.014	0.077 ± 0.007*	<0.001
Muscle	0.008 ± 0.001	0.011 ± 0.008	0.009 ± 0.002	0.010 ± 0.000	NS
Thymus	0.031 ± 0.004	0.041 ± 0.007	0.065 ± 0.012*	0.068 ± 0.011*	<0.001
Spleen	1.321 ± 0.183	2.111 ± 0.432*	2.410 ± 0.463*	2.355 ± 0.157*	0.001
BM	0.621 ± 0.048	1.237 ± 0.193*	1.493 ± 0.429*	2.048 ± 0.521*	<0.001
Liver	0.586 ± 0.042	0.740 ± 0.111	0.743 ± 0.204	0.669 ± 0.087	NS
Kidney	8.317 ± 0.295	6.897 ± 0.968	5.958 ± 1.452*	5.945 ± 0.583*	0.002
TBR	1.306 ± 0.217	1.197 ± 0.288	1.281 ± 0.312	2.052 ± 0.164*	<0.001
TMR	5.908 ± 0.839	5.873 ± 2.692	5.733 ± 1.690	7.528 ± 0.586*	<0.001

*$P < 0.05$ compared with control groups.
K–W = Kruskal–Wallis test; NS = not significant; BM = bone marrow; TBR = tumor-to-blood ratio; TMR = tumor-to-muscle ratio.
Data are (%ID/g) × kg (mean ± SD) except TBR and TMR.

TABLE 2
Weight of Organs

Height	Time after cyclophosphamide treatment (h) (n = 5)				P (K–W)
	0 (control)	4	12	20	
Whole body	252.4 ± 21.34	247.2 ± 17.73	251.4 ± 15.21	248.6 ± 13.52	NS
Tumor	0.964 ± 0.181	0.940 ± 0.265	1.031 ± 0.147	0.952 ± 0.130	NS
Muscle	1.041 ± 0.541	1.036 ± 0.295	1.264 ± 0.288	1.169 ± 0.102	NS
Thymus	0.522 ± 0.066	0.454 ± 0.139	0.411 ± 0.058	0.312 ± 0.066	<0.01
Spleen	0.723 ± 0.095	0.549 ± 0.094	0.433 ± 0.061	0.392 ± 0.034	<0.01
Liver	3.343 ± 0.479	3.395 ± 0.394	3.956 ± 0.828	3.446 ± 0.371	NS
Kidney	1.713 ± 0.141	1.755 ± 0.164	1.810 ± 0.138	1.838 ± 0.056	NS

K–W = Kruskal–Wallis test; NS = not significant.
Data are in grams (mean ± SD).

T/B ratios of ^{99m}Tc-annexin V were 1.197 ± 0.288, 1.281 ± 0.312, and 2.052 ± 0.164 at 4, 12, and 20 h after treatment compared with the control value of 1.306 ± 0.217. The T/M ratios were 5.908 ± 0.839, 5.873 ± 2.692, 5.733 ± 1.690, and 7.528 ± 0.586 in the control group at 4, 12, and 20 h respectively, after chemotherapy. The T/B and T/M ratios in the treated group 20 h after chemotherapy were significantly higher than those in the control group ($P < 0.05$). The changes over time were statistically significant for all ratios. The kidneys showed the highest radioactivity at all time points, followed (in decreasing order) by the spleen, bone marrow, liver, thymus, blood, and muscle. Radioactivity in the spleen, bone marrow, and thymus was significantly higher in the treated group than that in the control group, but radioactivity in the liver, blood, and muscle showed no definite change after chemotherapy. The weight of tumor was not affected statistically by cyclophosphamide treatment, but that of the spleen and thymus significantly decreased with time after chemotherapy (Table 2).

The rates of TUNEL-positively stained cells increased during the interval of observation. In control, 4, 12, and 20 h after chemotherapy, TUNEL-positive cells were 4.6% ± 0.7%, 6.4% ± 2.2%, 8.1% ± 1.8%, and 8.3% ± 1.6%, respectively (Fig. 1).

The rates of caspase-3–positively stained cells in the control, 4, 12, and 20 h after chemotherapy were 3.1% ± 2.1%, 4.2% ± 1.3%, 4.5% ± 1.4%, and 6.5% ± 2.3%, respectively. The rate at 20 h was significantly higher than that in the control group (Fig. 1).

DISCUSSION

The accumulation of ^{99m}Tc-annexin V in KDH-8 tumor tissue significantly increased at 20 h but not at 4 or 12 h after a single dose of cyclophosphamide. The T/B and T/M ratios also showed the same trend. The increase in the rate of tracer uptake was consistent with the rate of apoptotic cells determined by TUNEL and caspase-3 immunostaining before tumor regression occurred. It is also important to note that the increase in both the rate of uptake and the ratio of ^{99m}Tc-annexin V occurred well before tumor regression. Thus, the detection of apoptotic tumor response required 20 h after a single dose of cyclophosphamide in this experimental model. The near doubling of ^{99m}Tc-annexin V up-

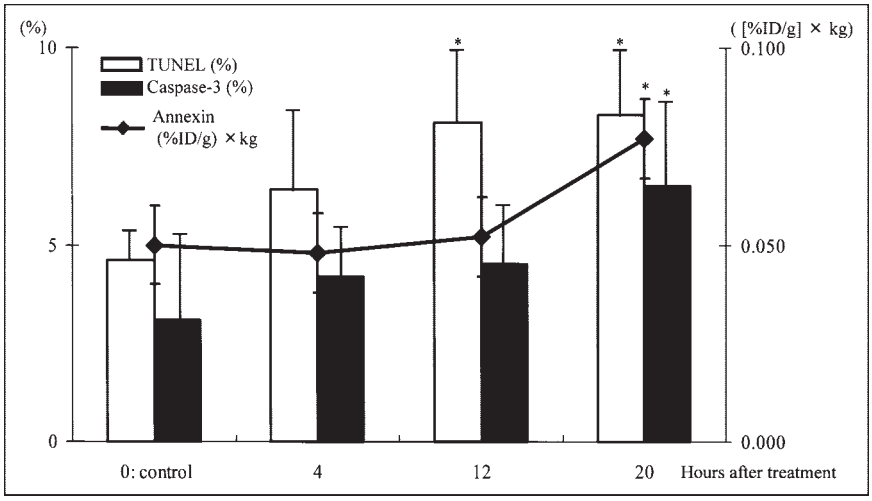

FIGURE 1. Radioactivity and rates of positively stained cells. *$P < 0.05$ compared with control group.

take in the tumor, T/B, and T/M ratios parallels the near doubling of the numbers of both TUNEL- and caspase-3–positively stained cells. This suggests that the in vivo imaging technique can provide a good reflection of the onset of apoptosis.

One of the earliest events in apoptosis is the externalization of PS, a membrane phospholipid normally restricted to the inner leaflet of the lipid bilayer (*6,27*). ^{99m}Tc-Annexin V can bind to PS with a high affinity depending on the Ca^{2+} concentration (*35*). According to previous reports, there are at least 2 peaks of PS expression (*27,36*). The early one appears within 1 h of chemotherapy initiation, and the second appears approximately 24–72 h after the completion of treatment (*27,36,37*). Blankenberg observed an increase in ^{99m}Tc-annexin V level 1 h after cyclophosphamide treatment of murine lymphoma but, paradoxically, there was no loss of lymphoma cells (*27*). Our current results showed no significant change in both the rate of ^{99m}Tc-annexin V uptake and the numbers of TUNEL- and caspase-3–positively stained cells 4 h after a single dose of cyclophosphamide. Furthermore, there were no definite morphologic changes 4 h after chemotherapy. Our recent study was designed to detect chemotherapy-induced apoptosis at the second peak of PS expression in a clinical setting. We consider that it may be too late to detect apoptosis 4 h after the chemotherapy even when we take 4-hydroxycyclophosphamide into consideration. However, the second peak of PS expression did not appear 4 and 12 h after the chemotherapy. These results imply that detection protocols should focus on the second peak of PS exposure, since the first peak of PS expression does not always reflect tumor apoptosis.

Blankenberg et al. reported that the second peak of ^{99m}Tc-annexin V uptake is also expected to occur hours later, immediately before the loss of the bulk of tumor cells due to apoptosis. They also reported an increase in ^{99m}Tc-annexin V uptake rate in the spleen and bone marrow as early as 8 h after cyclophosphamide treatment. This increased uptake rate lasted approximately 2 d (*12*). Our results confirmed that the rate of ^{99m}Tc-annexin V uptake also significantly increased in the tumor tissue, bone marrow, spleen, and other chemosensitive organs such as the thymus. Although the weights of the organs such as bone marrow, thymus, and spleen significantly decreased, the weight of tumor itself did not change. This phenomenon indicated that KDH-8 tumor was less chemosensitive than the hematopoietic organs.

Cyclophosphamide is an alkylating agent, which exerts its cytotoxic effect by alkylating 7 nitrogens of guanine in tumor DNA predominantly. Methylated DNAs prevent cell proliferation. The metabolic activation to 4-hydroxycyclophosphamide is required for its cytotoxic efficacy. This metabolite prevents cells, including hepatoma, from proliferating by arresting the cell cycle at the G2 phase. Higher doses of cyclophosphamide also prevent cell proliferation at the S phase and interrupt DNA synthesis (*34*). However, the efficacy of cyclophosphamide against KDH-8 tumor is not necessarily clear, and further studies are required to clarify this point. In contrast, clinical and experimental trials show that the degree of cancer apoptosis initiated by chemotherapy using cyclophosphamide correlates with tumor regression and prognosis. Mochizuki et al. reported the high correlation between the rate of TUNEL-positively stained and the uptake of ^{99m}Tc-annexin V (*20*). Therefore, we considered ^{99m}Tc-annexin V as a noninvasively monitoring tool to predict the therapeutic outcome. Antineoplastic agents induce apoptosis because the DNA damage leads to inhibition of the antiapoptotic molecules such as Bcl-2 and to product cytokines such as interleukin 2 and tumor necrosis factor α (TNF-α) (*38*). These molecules activate caspase-3 and, consequently, apoptosis occurs. We observed a significant increase of the rate of caspase-3–positive cells after cyclophosphamide treatment. Additionally, apoptosis of KDH-8 cells has been reported to depend on an increase in TNF-α (*39*). The apoptotic mechanism in KDH-8 cells induced by cyclophosphamide seems to be similar to that of other cancer cells, although the particular molecular mechanism is unclear.

This study showed that the caspase-3 expression level is concordant with the accumulation of ^{99m}Tc-annexin V. In contrast, the increase in the rate of TUNEL-positively stained cells tended to precede the increase in annexin binding. Unfortunately, the precise mechanism underlying this phenomenon is unclear. We speculate that this may be attributed primarily to DNA scission by cyclophosphamide, an alkylating agent. The cytotoxic effect occurs mainly by alkylating DNA as described, but the drug can also cut DNA strands directly (*34*). This DNA damage may influence the rates of TUNEL-positively stained cells, because the fragments of DNA cut by cyclophosphamide reacted during TUNEL, preceding apoptosis. Therefore, it is important to evaluate and correlate this with the extent of necrosis histologically. In the present study, the cells were considered "positive" when the nuclei were intensely stained by TUNEL for DNA fragmentation. Necrotic cells can be excluded on the basis of cytoplasmic staining and morphologic changes (e.g., pyknosis, nuclear fragmentation, cytoplasmic swelling, and presence of apoptotic bodies). In our experimental model, the weight of tumor did not decrease and the amount of the necrotic changes was small. Consequently, we considered the influence of necrosis to be limited or negligible in our experimental model. If the DNA ladder directly fragmented by cyclophosphamide is present in the nuclei, it is difficult to exclude necrosis strictly by TUNEL evaluation. On the other hand, caspase-3 staining cannot be easily affected by necrotic tissue (*40*).

In the present study, the T/M ratios are rather high even in the control rats, which can be ascribed to apoptosis in the control tumor. Tumor suppressor genes (e.g., p53) induce the apoptosis of cancer cells without chemotherapy (*38*). Further study, including scintigraphic imaging, is warranted to clarify the time course of apoptosis induced by repetitive chemotherapy. These data suggest that in a clinical setting, it is appropriate to wait for 1 or 2 d after a single dose of

chemotherapy when evaluating and imaging the apoptotic reaction using ^{99m}Tc-annexin V.

ACKNOWLEDGMENTS

The authors are grateful to Professors Shinzo Nishi, Kazuo Miyasaka, and Toshiyuki Ohnishi of the Central Institute of Isotope Science, Hokkaido University, for supporting this work. The authors also thank Koutaro Suzuki, Hidenori Katsuura, Hidehiko Omote, and Hiroshi Arai of the Facility of Radiology, Hokkaido University Medical Hospital, for assistance.

REFERENCES

1. Kerr JF, Wyllie AH, Currie AR. Apoptosis: a basic biological phenomenon with wide-ranging implications in tissue kinetics. *Br J Cancer.* 1972;26:239–257.
2. Thompson BC. Apoptosis in the pathogenesis and treatment of disease. *Science.* 1995;267:1456–1462.
3. Blankenberg F, Narula J, Strauss HW. In vivo detection of apoptotic cell death: a necessary measurement for evaluating therapy for myocarditis, ischemia, and heart failure. *J Nucl Cardiol.* 1999;6:531–539.
4. Post AM, Katsikis PD, Tait JF, et al. Imaging cell death with radiolabeled annexin V in an experimental model of rheumatoid arthritis. *J Nucl Med.* 2002;43:1359–1365.
5. Blankenberg FG, Tait J, Ohtsuki K, et al. Apoptosis: the importance of nuclear medicine. *Nucl Med Commun.* 2000;21:241–250.
6. Verhoven B, Schlegel RA, Williamson P. Mechanisms of phosphatidylserine exposure, a phagocyte recognition signal, on apoptotic T lymphocytes. *J Exp Med.* 1995;182:1597–1601.
7. Thiagarajan P, Tait JF. Binding of annexin V/placental anticoagulant protein I to platelets: evidence for phosphatidylserine exposure in the procoagulant response of activated platelets. *J Biol Chem.* 1990;265:17420–17423.
8. Tait JF, Gibson D, Fujikawa K. Phospholipid binding properties of human placental anticoagulant protein-I, a member of the lipocortin family. *J Biol Chem.* 1989;264:7944–7949.
9. Tait JF, Gibson D. Measurement of membrane phospholipid asymmetry in normal and sickle-cell erythrocytes by means of annexin V binding. *J Lab Clin Med.* 1994;123:741–748.
10. Wood BL, Gibson DF, Tait JF. Increased phosphatidylserine exposure in sickle cell disease: flow-cytometric measurement and clinical associations. *Blood.* 1996; 88:1873–1880.
11. Reutelingsperger CP, Dumont E, Thimister PW, et al. Visualization of cell death in vivo with annexin A5 imaging protocol. *J Immunol Methods.* 2002;265:123–132.
12. Blankenberg FG, Naumovski L, Tait JF, Post AM, Strauss HW. Imaging cyclophosphamide-induced intramedullary apoptosis in rats using ^{99m}Tc-radiolabeled annexin V. *J Nucl Med.* 2001;42:309–316.
13. Blankenberg FG, Katsikis PD, Tait JF, et al. In vivo detection and imaging of phosphatidylserine expression during programmed cell death. *Proc Natl Acad Sci USA.* 1998;95:6349–6354.
14. Blankenberg FG, Katsikis PD, Tait JF, et al. Imaging of apoptosis (programmed cell death) with ^{99m}Tc annexin V. *J Nucl Med.* 1999;40:184–191.
15. Ohtsuki K, Akashi K, Aoka Y, et al. Technetium-99m HYNIC-annexin V: a potential radiopharmaceutical for the in-vivo detection of apoptosis. *Eur J Nucl Med.* 1999;26:1251–1258.
16. Tait JF, Blankenberg FG, Strauss HW, et al. Development and characterization of annexin V mutants with endogenous chelation sites for ^{99m}Tc. *Bioconjug Chem.* 2000;11:918–925.
17. Joseph B, Lewensohn R, Zhivotovsky B. Role of apoptosis in the response of lung carcinomas to anti-cancer treatment. *Ann NY Acad Sci.* 2000;926:204–216.
18. Fromigue O, Lagneaux L, Body JJ. Bisphosphonates induce breast cancer cell death in vitro. *J Bone Miner Res.* 2000;15:2211–2221.
19. Amezcua CA, Lu JJ, Felix JC, Stanczyk FZ, Zheng W. Apoptosis may be an early event of progestin therapy for endometrial hyperplasia. *Gynecol Oncol.* 2000;79: 169–176.
20. Mochizuki T, Kuge Y, Zhao S, et al. Detection of apoptotic tumor response in vivo after a single dose of chemotherapy with ^{99m}Tc-annexin V. *J Nucl Med.* 2003;44:92–97.
21. Vriens PW, Blankenberg FG, Stoot JH, et al. The use of 99m technetium labeled annexin V for in vivo imaging of apoptosis during cardiac allograft rejection. *J Thorac Cardiovasc Surg.* 1998;116:844–853.
22. Hofstra L, Liem IH, Dumont EA, et al. Visualisation of cell death in vivo in patients with acute myocardial infarction. *Lancet.* 2000;356:209–212.
23. Blankenberg FG, Robbins RC, Stoot JH, et al. Radionuclide imaging of acute lung transplant rejection with annexin V. *Chest.* 2000;117:834–840.
24. Ogura Y, Krams SM, Martinez OM, et al. Radiolabeled annexin V imaging: diagnosis of allograft rejection in an experimental rodent model of liver transplantation. *Radiology.* 2000;214:795–800.
25. D'Arceuil H, Rhine W, de Crespigny A, et al. ^{99m}Tc annexin V imaging of neonatal hypoxic brain injury. *Stroke.* 2000;32:2692–2700.
26. Yang DJ, Azhdarina A, Wu P, et al. In vivo and in vitro measurement of apoptosis in breast cancer cells using ^{99m}Tc-EC-annexin V. *Cancer Biother Radiopharm.* 2001;16:73–83.
27. Blankenberg FG. To scan or not to scan: it is a question of timing—technetium-99m annexin V radionuclide imaging assessment of treatment efficacy after one course of chemotherapy. *Clin Cancer Res.* 2002;8:2757–2758.
28. Belhocine T, Steinmetz N, Hustinx R, et al. Increased uptake of the apoptosis-imaging agent ^{99m}Tc-recombinant human annexin V in human tumors after one course of chemotherapy as a predictor of tumor response and patient prognosis. *Clin Cancer Res.* 2002;8:2766–2774.
29. Van de Wiele C, Lahorte C, Vermeersch H. Quantitative tumor apoptosis imaging using technetium-99m-HYNIC annexin V single photon emission computed tomography. *J Clin Oncol.* 2003;21:3483–3487.
30. Zhao S, Kuge Y, Tsukamoto E, et al. Effects of insulin and glucose loading on FDG uptake in experimental malignant tumors and inflammatory lesions. *Eur J Nucl Med.* 2001;28:730–735.
31. Tait JF, Engelhardt S, Smith C, Fujikawa K. Prourokinase-annexin V chimeras: construction, expression, and characterization of recombinant proteins. *J Biol Chem.* 1995;270:21594–21599.
32. Tait JF, Smith C. Site-specific mutagenesis of annexin V: role of residues from Arg-200 to Lys-207 in phospholipid binding. *Arch Biochem Biophys.* 1991;288: 141–144.
33. Gavrieli Y, Sherman Y, Ben-Sasson SA. Identification of programmed cell death in situ via specific labeling of nuclear DNA fragmentation. *J Cell Biol.* 1992; 119:493–501.
34. Chabner BA, Allegra CJ, Curt GA, Calabresi P. Antineoplastic agents. In: Chabner BA, Allegra CJ, Curt GA, Calabresi P, eds. *Goodman and Gilman's The Pharmacological Basis of Therapeutics*. 9th ed. New York, NY: McGraw-Hill; 1996:1233–1243.
35. Gerke V, Moss SE. Annexins: from structure to function. *Physiol Rev.* 2002;82: 331–371.
36. Dumont EA, Reutelingsperger CP, Smits JF, et al. Real-time imaging of apoptotic cell-membrane changes at the single-cell level in the beating murine heart. *Nat Med.* 2001;7:1352–1355.
37. Green AM, Steinmetz ND. Monitoring apoptosis in real time. *Cancer J.* 2002; 8:82–92.
38. Raff M. Cell suicide for beginners. *Nature.* 1998;396:119–122.
39. Matsushita K, Kobayashi M, Hosokawa M. ONO-4007, a synthetic lipid A analog, induces Th1-type immune response in tumor eradication and restores nitric oxide production by peritoneal macrophages. *Int J Oncol.* 2003;23:489–493.
40. Stadelmann C, Lassmann H. Detection of apoptosis in tissue sections. *Cell Tissue Res.* 2000;301:19–31.

JNM The Journal of NUCLEAR MEDICINE

Time Course of Apoptotic Tumor Response After a Single Dose of Chemotherapy: Comparison with ^{99m}Tc-Annexin V Uptake and Histologic Findings in an Experimental Model

Toshiki Takei, Yuji Kuge, Songji Zhao, Masayuki Sato, H. William Strauss, Francis G. Blankenberg, Jonathan F. Tait and Nagara Tamaki

J Nucl Med. 2004;45:2083-2087.

The Journal of Nuclear Medicine is published monthly.
SNMMI | Society of Nuclear Medicine and Molecular Imaging
1850 Samuel Morse Drive, Reston, VA 20190.
(Print ISSN: 0161-5505, Online ISSN: 2159-662X)

SNMMI SOCIETY OF NUCLEAR MEDICINE AND MOLECULAR IMAGING